Preprints of the 21st IFAC World Congress (Virtual)
Berlin, Germany, July 12-17, 2020

Hybrid Output Regulation of DC-DC Converter for Dynamic Wireless Charging System

Mengting Zhang * **Lorenzo Marconi** ** **Zhitao Liu** *
Hongye Su *

* *Department of Control Science and Engineering, Zhejiang University, Hangzhou, P.R.China (e-mail: 11832053@zju.edu.cn; ztliu@zju.edu.cn; hysu@iipc.zju.edu.cn)*
** *CASY-DEI, University of Bologna, Bologna, Italy. (e-mail: lorenzo.marconi@unibo.it)*

Abstract: This paper illustrates a control strategy for voltage regulation problem of DC-DC converter in dynamic wireless charging applications. The control goal is to compensate for the disturbances on the input voltage of the DC-DC converter that changes periodically due to the motion of the electric vehicle assumed to have a constant speed. The paper aims at comparing two different control solutions based on continuous and hybrid internal model-based regulators. According to the relative distance of the transmitter coils the fluctuation of the input voltage is approximated as a continuous-time or a spline-based periodic signal and internal model-based solutions, which are continuous time or hybrid according to the fluctuation modelling, are proposed to compensate for such a disturbance. The control performance of the proposed control schemes are tested through simulation by showing how, as long as the relative distance between the coils increases, the more involved hybrid solutions improve the performances when compared with the more simple continuous-time ones.

Keywords: Hybrid control, output regulation, dynamic wireless charging system

1. INTRODUCTION

In recent years Wireless Power Transfer technology is becoming more attractive worldwide by gaining popularity in various type of applications, especially in electric vehicles. In this relevant application context the key challenges in the actual battery technology are inadequate storage capacity asking for efficient recharging systems. To compensate for the slow development of current battery technology, Dynamic Wireless Charging (DWC) technology has developed (see Li et al. (2015), Bertoluzzo et al. (2016) and Guo et al. (2016)). The development of DWC technologies has the potential to address the limitation of charging time and of the actual charging infrastructure. There are two major types of DWC typically referred to as centralised and segmented track (Ahmad et al. (2018)). As for the segmented track type, which is the one addressed in this paper, each segment of the track has a Transmitter (Tx) coil with all the coils that are coupled and properly synchronised by a sequence logic which is designed to optimise the power supply to the Receiver (Rx) coil onboard of the electric vehicle. A graphical sketch of a typical DWC system for electric vehicles is shown in Fig. 1.

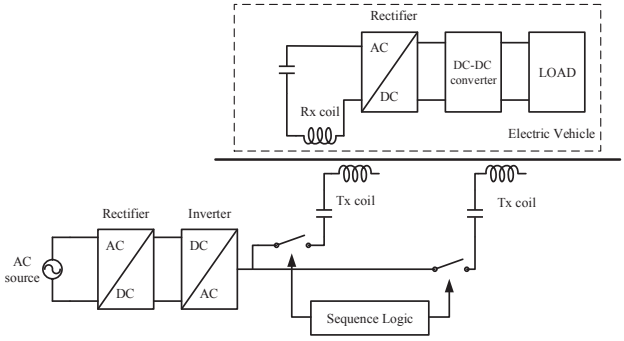

Fig. 1. Block diagram of a dynamic wireless charging system

A key component to regulate the output voltage to the load is the DC-DC converter. This component is subject to wide range disturbances requiring advanced control strategies to adjust its duty cycle and to enforce a stable output voltage to the load. More precisely, one of the most challenging problem in DWC systems is the variation of the mutual-inductance between the Tx and Rx coils caused by the coil misalignment while the vehicle is in motion (see Hwang et al. (2017) and Rakhymbay et al. (2018)). This problem results in the constantly varying input voltage of the DC-DC converter. In other words, when the Rx coil is precisely aligned to the top of Tx coil, the mutual-inductance reaches its highest point and thus the input

⋆ This work was supported in part by the National Key R&D Program of China (Grant NO.2018YFA0703800), Science Fund for Creative Research Group of the National Natural Science Foundation of China (Grant NO.61621002), Nation Natural Science Foundation of China (NSFC:61873233, 61633019), Fundamental Research Funds for the Central Universities.

voltage is the largest. In contrast, when the Rx coil moves to the middle between two next Tx coils, the input voltage drops. The fluctuation of the input voltage is periodic if the vehicle is moving at constant speed along the segmented track. To address such misalignment issue and regulate the output voltage of DWC system to a constant value, a sophisticated control problem at DC-DC converter level must be dealt with (see Lovison et al. (2017) and Qiang et al. (2017)).

In this paper, a solution to the voltage regulation problem of DC-DC converters based on output regulation theory is proposed. We first present a modelling analysis of the periodic disturbance induced by the input voltage fluctuations. The analysis will show that the nature of the disturbance is strongly affected by the coils relative distance and by the vehicle speed. A harmonic-based approximation with known frequencies and unknown amplitude and phase and a spline-based polynomial approximation, with known transition times between different polynomials but unknown polynomial coefficients, are both effective to capture the behaviour of the disturbance. We then design controllers for regulating the output voltage to a constant value robustly with respect to the input disturbance induced by the voltage fluctuations and to parametric coefficients of the DC-DC converter. The solution will necessarily rely on control structures embedding an internal model of the disturbance, leading to hybrid internal model-based solutions as long as the coil misalignment is large.

The problem of output regulation has been intensively studied in the linear (Francis and Wonham (1976) and Francis (1975)) as well as nonlinear (Byrnes et al. (2002)) continuous-time contexts. Meanwhile, hybrid control systems have attracted a lot of interest both at academic and industry level (Goebel et al. (2012)). In the context of hybrid systems a theory of output regulation was presented in Marconi and Teel (2010) (see also Cox et al. (2011b), Cox et al. (2011a)). A significant progress of *robust* output regulation for a class of hybrid linear systems and exosystems has been given in Marconi and Teel (2013). That paper developed key concepts and tools for the hybrid setting and proposed constructive design procedures for a hybrid internal model-based regulator yielding asymptotic regulation in a systematic way in presence of uncertainties on the regulated system.

In this paper we adopt standard theory of continuous-time output regulation and hybrid output regulation to address the problem at hand. The goal of the work is to show the effectiveness of the internal model-based control schemes for this problem by also comparing the performances of the different solutions in relation to the relative distance of the coils and the vehicle speed.

2. MODEL OF THE DYNAMIC WIRELESS CHARGING SYSTEM

2.1 Modeling for DC-DC Converter

We adopt the state space average method proposed in Suntio (2009) to model voltage-mode (VM) buck converter in continuous conduction mode (CCM). A typical buck converter is shown in Fig. 2 where i_L denotes the current through inductor L, u_C the voltage of filter capacitor C,

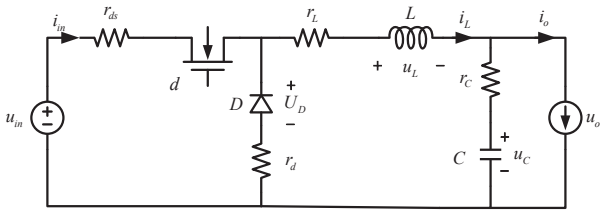

Fig. 2. Typical buck converter

u_{in} the input voltage of buck converter, i_o the output current of buck converter, d the duty cycle of buck converter, u_o the output voltage of buck converter and u_{ref} the reference output voltage of buck converter respectively. According to state space average method, these variables can be replaced by a DC term plus an AC term. In the following we shall denote a generic variable by $v = V + \hat{v}$ where V represents the DC value in steady-state condition while $\hat{v}$ is the AC values corresponding to the dynamic behavior. Moreover, to better analyse the modeling of DC-DC converter, the parasitic circuit elements such as the resistances and the diode forward voltage U_D are considered. The values assumed for the component parameters are listed in Table 1.

Table 1. System parameters for buck converter

System parameter	Value
Input Voltage U_{in}	300V
Output Voltage U_o	30V
Reference Output Voltage U_{ref}	30V
Filter Inductor L	2.76mH
Filter Capacitor C	470μF
Equivalent Serial Resistance (ESR) r_C	0.027Ω
Inductor Parasitic Resistance r_L	0.041Ω
Diode Parasitic Resistance r_D	0.037Ω
MOSFET Parasitic Resistance r_ds	0.045Ω
Diode Forward Voltage U_D	0.49V
Load Current I_o	10A
Operating Switch Frequency f_s	20kHz

By defining $u = \hat{d} \in \mathbb{R}$ as the control input, $x = [\hat{i}_L \quad \hat{u}_C]^T \in \mathbb{R}^2$ the state vector, $y = \hat{u}_o \in \mathbb{R}$ the measured output, $\mathrm{d} = [\hat{u}_{in} \quad \hat{i}_o]^T \in \mathbb{R}^2$ the disturbance, and $e \in \mathbb{R}$ the regulation error between output voltage $y = \hat{u}_o$ and the reference $r = \hat{u}_{ref}$, respectively, the standard state space model of buck converter reads as

$$\begin{cases} \dot{x} = Ax + Bu + E\mathrm{d} \\ y = C_y x + D_y u + F\mathrm{d} \\ e = y - r. \end{cases} \tag{1}$$

in which the system matrices are

$$\begin{aligned} A &= \begin{bmatrix} -\dfrac{r_L + Dr_{ds} + (1-D)r_d + r_C}{L} & -\dfrac{1}{L} \\ \dfrac{1}{C} & 0 \end{bmatrix} \\ B &= \begin{bmatrix} \dfrac{U_{in} + U_D + (r_d - r_{ds})I_L}{L} \\ 0 \end{bmatrix} \\ C_y &= [r_C \quad 1] \quad \mathrm{D_y} = 0 \\ E &= \begin{bmatrix} \dfrac{D}{L} & \dfrac{r_C}{L} \\ 0 & -\dfrac{1}{C} \end{bmatrix} \quad F = [0 \quad -r_C] \end{aligned} \tag{2}$$

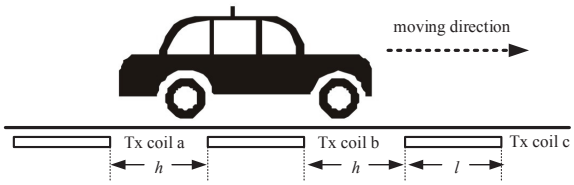

Fig. 3. Diagram of moving vehicle along a segmented track

where D represents the ideal steady state for the control input, namely the duty cycle of the PWM. The variable e is a regulation error that must be steered to zero by compensating for the effect of the disturbance d.

2.2 Approximating the input voltage disturbance

In this section we analyse the periodic fluctuation of input voltage $\hat{u}_{in}$ of the DC-DC converter by simulating three scenarios characterised by different gaps between subsequent Tx coils. A classical arrangement of Tx coils for segmented dynamic wireless EV charging system is shown in Fig. 3, with three segmented Tx coils and one electric vehicle. The gap h between two subsequent segmented Tx coils is clearly an important factor of power transfer efficiency (see Bertoluzzo et al. (2016)). In the following we simulate three different scenarios characterised by taking the gap h between subsequent Tx coils to be as 100%, 200% and 300% of coil length l and considering a constant vehicle speed.

The simulation is performed by adopting the electromagnetic analysis tool ANSYS MAXWELL (Chen and Liu (2014)) and considering a double-D coils in this segmented dynamic wireless charging system. The behaviour of the input voltage disturbance as a function of the longitudinal misalignment in the three indicated scenarios is shown in Fig. 4. As expected, the DC voltage in the receiver side reaches its maximum when the Rx coil is precisely aligned to the top of each Tx coil. Then, when the vehicle moves forward to the next Tx coil, the input voltage gradually decreases and reaches its minimum value. The change of input voltage is clearly periodic if the vehicle is moving at constant speed along the segmented track.

To pave the way to the control design, in the next part of the section we look for approximations of $\hat{u}_{in}(t)$ that are exosystem-generated. The goal is to obtain an appropriate (approximated) model of the disturbance to be embedded in the controller as internal model in order to reduce its effect on the regulated output. We adopt two approximated functions at increasing levels of complexity that are in principle able to capture the main behaviour indicated in Fig. 4. The plot on the top of Fig. 4 suggests that when the relative distance between coils is small relatively to the vehicle speed, the disturbance is well approximated with a periodic continuous-time signal with known frequency (dependent on distance h and on the speed) and unknown amplitude and phase (depending on the vehicle initial position and other physical parameters such as mutual inductance typically unknown). An exosystem able to generate such a behaviour is given by

$$\dot{\zeta} = S_1\zeta\,, \quad \hat{u}_{in,1} = \Gamma_1\zeta\,, \quad \zeta \in \mathbb{R}^{2N_f} \tag{3}$$

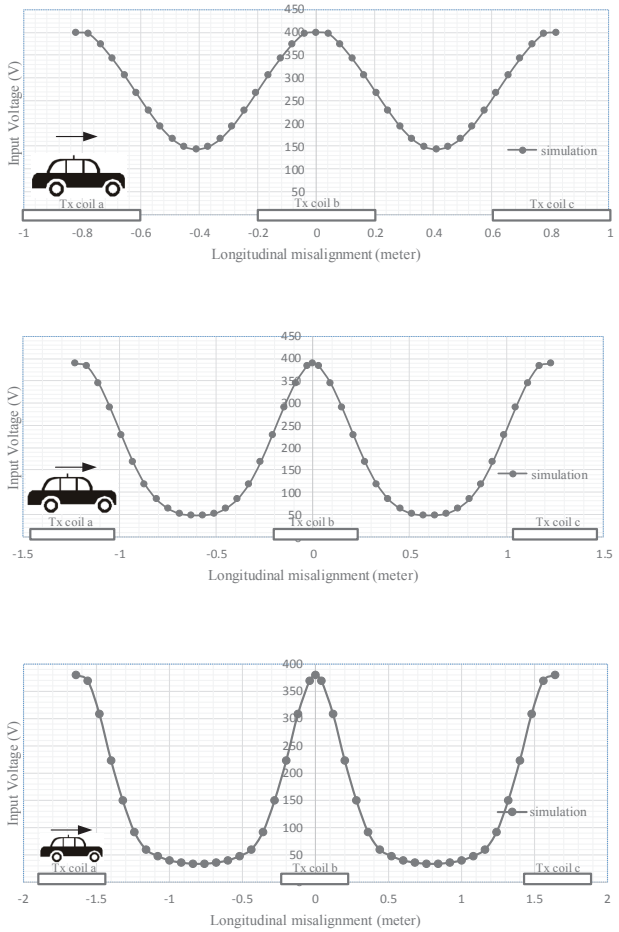

Fig. 4. Input voltage disturbance on the receiver side: (a)$h = l$; (b)$h = 2l$; (c)$h = 3l$.

in which S_1 is a critically stable matrix with N_f complex pairs of eigenvalues at $\pm j\Omega_i$ ($\Omega_i, i = 1, ..., N_f$ being the disturbance frequencies) and $\Gamma_1 = (\gamma_1, \gamma_2, ..., \gamma_{2N_f}), \gamma_{2i} = 0, \gamma_{2i+1} = 1, i = 1, ..., N_f$.

Fig. 5 shows, in the three simulated scenarios, the approximation error (as a function of the longitudinal misalignment) between the three disturbances plotted in Fig. 4 and the output of the exosystem (3) when the initial condition of the latter is taken to match the main frequencies of the signals. Here, we fixed the number of N_f in the three simulated scenarios as $N_f = 2$. The approximation is perfect when $h = l$, while it clearly degrades when the coil distance increases.

In order to improve the approximation in all the three scenarios, we approximate the input voltage curve as a spline-based disturbance. With an eye to Fig. 4, the periodic input voltage $\hat{u}_{in}(t)$ can be thought of as obtained by concatenating a basic signal $\mathcal{B}(t)$as

$$\hat{u}_{in}(t) = \mathcal{B}(t - iT), \quad i = \lfloor \frac{t}{T} \rfloor \quad t \geq 0, \quad T > 0$$

where the period is given by T and $\mathcal{B} : [0, T] \to \mathbb{R}$ is a sufficiently smooth function. $\mathcal{B}(t)$ can be taken as a spline function that passes through N equally spaced points $\{p_1, p_2, ..., p_N\}$ at time instances $\{t_1, t_2, ..., t_N\}$, namely

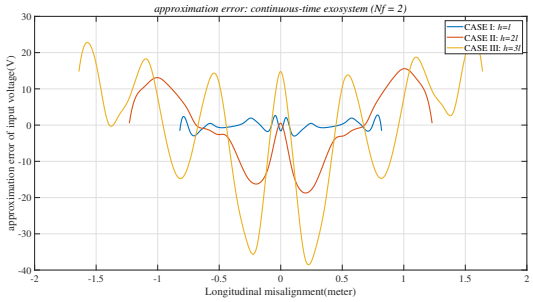

Fig. 5. Approximation error of continuous-time exosystem

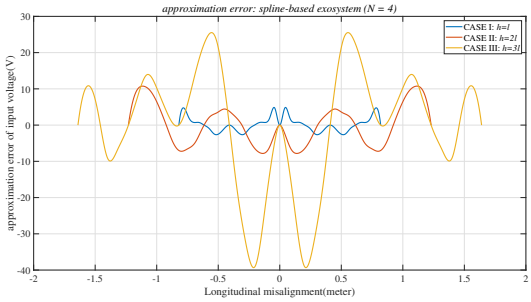

Fig. 6. Approximation error of spline-based exosystem

$\mathcal{B}(t_k) = p_k, t_{k+1} - t_k = T/N, k = 1, ..., N$ with $t_1 = 0$. The basic theory of spline interpolation (Schumaker (2007)) is then used to interpolate N polynomials $\mathcal{P}_k(t) : [t_k, t_{k+1}] \to \mathbb{R}$ such that $\mathcal{P}_k(t_k) = p_k, \mathcal{P}_k(t_{k+1}) = p_{k+1}, k = 1, ..., N$. Then, by following the design method of exosystem generating splines presented in (Cox et al., 2012), it turns out that, by letting $P_s = (p_3 \ ... \ p_N \ p_1 \ p_2)$, $Q_1 = (1 \ 0_{1\times 3})$ and $S_0 \in \mathbb{R}^{4\times 4}$ whose elements are all zero except along the superdiagonal, the voltage disturbance can be approximated as the output of the following hybrid exosystem [1]

$$\left.\begin{aligned}\dot{\tau} &= 1\\ \dot{\zeta}_1 &= S_0\zeta_1\\ \dot{\zeta}_2 &= 0\end{aligned}\right\} (\tau,\zeta) \in [0,\tau_{max}]\times\mathbb{R}^{N+4}$$
$$\left.\begin{aligned}\tau^+ &= 0\\ \zeta_1^+ &= J_{11}\zeta_1 + J_{12}\zeta_2\\ \zeta_2^+ &= J_{22}\zeta_2\end{aligned}\right\} (\tau,\zeta) \in \{\tau_{max}\}\times\mathbb{R}^{N+4} \qquad (4)$$
$$\hat{u}_{in,2} = Q_1\zeta_1$$

where $\tau_{\max} = T/N$,

$$J_{11} = \begin{pmatrix} I_3 & 0_{3\times 1}\\ L_1 & \end{pmatrix} \quad J_{12} = \begin{pmatrix} 0_{3\times N}\\ L_2\end{pmatrix}$$
$$J_{22} = \begin{pmatrix} 0_{1\times N-1} & 1\\ I_{N-1} & 0_{N-1\times 1}\end{pmatrix}$$

with $L_2 = 6/\tau_{max}^3 P_s$ and

$$L_1 = \frac{-18}{\tau_{max}^3}Q_1 e^{-S_0\tau_{max}} + \frac{12}{\tau_{max}^3}Q_1 + \frac{-6}{\tau_{max}^2}Q_1 S_0 e^{-S_0\tau_{max}} + \frac{-18}{\tau_{max}^2}Q_1 S_0$$

In a more compact way the previous hybrid exosystem can be written as

$$\left.\begin{aligned}\dot{\tau} &= 1\\ \dot{\zeta} &= S_2\zeta\end{aligned}\right\} \quad (\tau,\zeta) \in [0,\tau_{max}]\times\mathbb{R}^{N+4}$$
$$\left.\begin{aligned}\tau^+ &= 0\\ \zeta^+ &= J_2\zeta\end{aligned}\right\} \quad (\tau,\zeta) \in \{\tau_{max}\}\times\mathbb{R}^{N+4} \qquad (5)$$
$$\hat{u}_{in,2} = \Gamma_2\zeta$$

where the matrices S_2, J_2 and Γ_2 and the state ζ are implicitly defined.

Fig. 6 shows, in the three simulated scenarios, the approximation error (as a function of the longitudinal misalignment) between the three disturbances plotted in Fig. 4 and the output of the exosystem (5) when the initial condition of the latter is taken to match the prescribed N points $\{p_1, p_2, ..., p_N\}$ of the basic signal $\mathcal{B}$. Here, we fixed the number of N as $N = 4$. Similarly to the continuous time case, the approximation also degrades when the coil distance increases.

Overall, by choosing N_f for continuous-time exosystem and N for spline-based exosystem appropriately, the continuous-time and hybrid approximated model are able to better capture the behaviour of the input voltage.

3. THE INTERNAL MODEL-BASED ROBUST REGULATOR

We build on the arguments presented in the previous section to design a robust controller embedding an internal model of the periodic disturbance. With an eye to (1), the goal of the controller is to let the regulated output y track a *constant* reference r by compensating for the effect of the disturbance $\mathrm{d}(t)$, the latter given by the periodic input voltage $\hat{u}_{in}(t)$ and the output current $\hat{i}_0$. Uncertainties that typically characterise the system are of different kinds. As for the periodic input voltage $\hat{u}_{in}(t)$, the scale and the phase of the signal are typically uncertain since they depend on the mutual inductance and on the vehicle position between coils. This uncertainty reflects in a lack of knowledge of the initial condition of the exosystem in the two approximation scenarios dealt with in the previous section. On the other hand, the frequency of the signal, depending on the speed of the vehicle and the geometry of the coils arrangement (i.e. h and l), can be assumed to be known. This, in turn, is reflected in the fact that the exosystem dynamics, captured by the matrices S_i, J_i, $i = 1, 2$, and by τ_{max} in the two addressed approximation scenarios, are known. As for the output current $\hat{i}_0$, it can be considered constant but unknown since its values is typically affected by the load. Overall, thus, the disturbance and the reference signal, in the two approximation settings presented in the previous section, can be compactly thought of as generated by an exosystem of the form

$$\left.\begin{aligned}\dot{\tau} &= 1\\ \dot{w} &= Sw\end{aligned}\right\} \quad (\tau,w) \in [0,\tau_{max}]\times\mathbb{R}^{n_w}$$
$$\left.\begin{aligned}\tau^+ &= 0\\ w^+ &= Jw\end{aligned}\right\} \quad (\tau,w) \in \{\tau_{max}\}\times\mathbb{R}^{n_w} \qquad (6)$$

$$\begin{pmatrix}\hat{u}_{in}\\ \hat{i}_0\end{pmatrix} = L_d w\,, \quad r = L_r w \qquad (7)$$

[1] We use the notation used for hybrid systems proposed in Goebel et al. (2012).

in which, in case $\hat{u}_{in}$ is modelled as in (3), $n_w = 2N_f + 2$, $w = \text{col}(w_1, w_2, w_3)$ with $w_1 \in \mathbb{R}^{2N_f}$, $w_2 \in \mathbb{R}$, $w_3 \in \mathbb{R}$, L_d and L_r are such that $L_d w = \text{col}(\Gamma_1 w_1, w_2)$, $L_r w = w_3$,

$$S := \begin{pmatrix} S_1 & 0_{2N_f \times 2} \\ 0_{2N_f \times 2} & 0_{2\times 2} \end{pmatrix} \quad J := I_{n_w} ,$$

with (S_1, Γ_1) introduced above, while, in case $\hat{u}_{in}$ is modelled as in (5), $n_w = N + 6$, $w = \text{col}(w_1, w_2, w_3)$ with $w_1 \in \mathbb{R}^{N+4}$, $w_2 \in \mathbb{R}$, $w_3 \in \mathbb{R}$, L_d and L_r are such that $L_d w = \text{col}(\Gamma_2 w_1, w_2)$, $L_r w = w_3$,

$$S := \begin{pmatrix} S_2 & 0_{N+4\times 2} \\ 0_{2\times N+4} & 0_{2\times 2} \end{pmatrix} \quad J := \begin{pmatrix} J_2 & 0_{N+4\times 2} \\ 0_{2\times N+4} & I_{2\times 2} \end{pmatrix}$$

with (S_2, J_2, Γ_2) introduced in the previous section. We observe that, in the first case, the exosystem is continuous time, namely the jump dynamics is fictitious ($J = I$ and $\tau_{\max}$ irrelevant). Furthermore, we observe that the above said uncertainties reflect in the fact that the initial condition $w(0)$ of the exosystem is not known.

Overall the regulated plant (1) with the external disturbance modelled as above can be written as

$$\left.\begin{aligned} \dot{\tau} &= 1 \\ \dot{w} &= Sw \\ \dot{x} &= Ax + Bu + Pw \end{aligned}\right\} \quad (\tau, w) \in [0, \tau_{max}] \times W$$
$$\left.\begin{aligned} \tau^+ &= 0 \\ w^+ &= Jw \\ x^+ &= Mx + Nw \end{aligned}\right\} \quad (\tau, w) \in \{\tau_{max}\} \times W \qquad (8)$$
$$e = C_e x + Q_e w$$

in which $C_e = C_y$, $P = EL_d$, $Q_e = FL_d - L_r$, $M = I_2$, $N = 0_{2\times n_w}$. We further observe that, in case the voltage disturbance is modelled as in (3), system (8) is indeed continuous-time, namely $J = M = I_2$, and the state of the system doesn't change during jumps ($w^+ = w$, $x^+ = x$, and the definition of τ_{max} is irrelevant).

In this context the problem is then to design a regulator of the form

$$\left.\begin{aligned} \dot{\tau} &= 0 \\ \dot{\xi} &= F_F \xi + G_F e \end{aligned}\right\} \quad (\tau, \xi) \in [0, \tau_{max}] \times \mathbb{R}^{n_\xi}$$
$$\left.\begin{aligned} \tau^+ &= 0 \\ \xi^+ &= F_J \xi + G_J e \end{aligned}\right\} \quad (\tau, \xi) \in \{\tau_{max}\} \times \mathbb{R}^{n_\xi} \qquad (9)$$
$$u = \Psi \xi + K e$$

such that for all initial conditions $(\tau(0), w(0), x(0), \xi(0)) \in [0, \tau_{max}] \times \mathbb{R}^{n_w} \times \mathbb{R}^2 \times \mathbb{R}^{n_\xi}$ the trajectories of the resulting closed-loop system (8)-(9) are bounded and the regulation error e converges to zero asymptotically. Such a controller becomes continuous-time in case $\hat{u}_{in}$ is approximated as in (3).

3.1 The regulator with continuous-time internal model

By considering the voltage disturbance modelled as in (3), we firstly consider the continuous-time system described by the flow dynamics of (8) and we design a continuous-time regulator embedding as internal model a copy of (3). Since the system in question has relative degree one between the input u and the error e and it is minimum-phase with respect to this input-output pair, by following the basic regulator theory the regulator takes the form

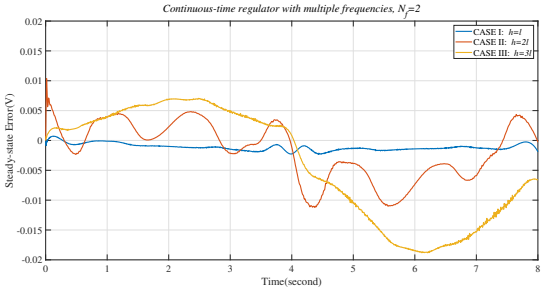

Fig. 7. Continuous-time internal model-based regulator. Steady-state error $e(t)$

$$\begin{aligned} \dot{\xi}_i &= \xi_{i+1} + h_i g^i e \\ \dot{\xi}_{n_w-1} &= \Phi \xi + h_{n_w-1} g^{n_w-1} e \\ u &= K_\xi \xi_1 + K_e e \end{aligned} \qquad (10)$$

in which, with h_i appropriately chosen and g sufficiently large, Φ fixed according to the characteristic polynomial of S, $K_e = -\kappa$ with κ a positive design parameter, and $K_\xi = -K_e$. It turns out (see Isidori et al. (2003)) that if κ is taken sufficiently large then the controller (10) solves the problem provided that w is generated as in (3).

The simulation results obtained with this controller in the three coil scenarios illustrated in Section 2.2 are presented in Fig. 7, showing the steady state errors. The results have been obtained by taking $\kappa = 1$, and h_i and g chosen so that the ξ subsystem is Hurwitz. As expected the closed-loop steady state performance deteriorates as the distance between the coils increases.

3.2 The regulator with hybrid internal model

In this part we consider the voltage disturbance as generated by the hybrid exosystem (5) and we propose a hybrid internal model based regulator by following the theory of Cox et al. (2016). By following that theory we let $\Pi_x : [0, \tau_{\max}] \mapsto \mathbb{R}^{2\times n_w}$ and $R : [0, \tau_{\max}] \mapsto \mathbb{R}^{1\times n_w}$ be the solution of the *hybrid regulator equations*

$$\begin{aligned} \frac{d\Pi_x(\tau)}{d\tau} &= A\Pi_x(\tau) - \Pi_x(\tau)S + P + BR(\tau) \\ 0 &= M\Pi_x(\tau_{\max}) - \Pi_x(0)J + N \\ 0 &= C\Pi_x(\tau) + Q \end{aligned} \qquad (11)$$

and we consider the regulator

$$\begin{aligned} \dot{\xi} &= F(\tau)\xi + G(\tau)u \qquad \xi \in \mathbb{R}^{N+6} \\ \xi^+ &= \Sigma_{\text{im}} \xi \\ u &= \Gamma(\tau)\xi + Ke \end{aligned} \qquad (12)$$

flowing and jumping according to the clock τ, in which $K = -\kappa$ with κ a design parameter, (F, G, Σ) is a triplet fulfilling the properties of Definition 2 in Cox et al. (2016). The regulator (12) entails the design of an asymptotic observer for the steady-state generator system. For details about the structure of (F, G, Σ), the interested reader is referred to Cox et al. (2016). As shown in that paper, since the flow dynamics have relative degree one between the input u and the error e and they are minimum-phase, the regulator (12) solves the problem at hand provided that the design parameter κ is kept sufficiently large and the voltage disturbance is generated by (5).

The steady state errors obtained with this controller in the three coil scenarios illustrated in Section 2.2 are presented

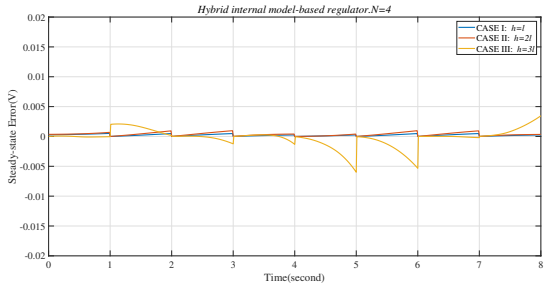

Fig. 8. Hybrid internal model-based regulator. Steady-state error $e(t)$

in Fig. 8. The results have been obtained by taking $\kappa = 1$. As expected the hybrid regulator improves the closed-loop steady state performances greatly when compared with the continuous-time one although it also deteriorates as the distance between the coils increases.

4. CONCLUSIONS

In this paper, a novel control method for buck-type DC-DC converter in the dynamic wireless charging scenario is presented. The theoretical background is based on the output regulation theory under the hypothesis that the input voltage fluctuation of DC-DC converter due to the motion of the electric vehicle can be approximated as a continuous-time or a spline-based periodic disturbance. The continuous-time and hybrid internal model-based regulators have been designed to compensate for such a disturbance according to the disturbance modelling. The simulation results shows that the more involved hybrid solutions improve the closed-loop performances when compared with the more simple continuous-time ones as the relative distance between the coils increases. Future works will deal with developing solutions that are robust to also possible uncertainties of the plant and to deal with the other DC-DC converters that are non minimum-phase. Experimental activities are also planned.

REFERENCES

Ahmad, A., Alam, M.S., and Chabaan, R. (2018). A comprehensive review of wireless charging technologies for electric vehicles. *IEEE Transactions on Transportation Electrification*, 4(1), 38–63.

Bertoluzzo, M., Buja, G., and Dashora, H.K. (2016). Lumped track layout design for dynamic wireless charging of electric vehicles. *IEEE Transactions on Industrial Electronics*, 63(10), 6631–6640.

Byrnes, C.I., Priscoli, F.D., and Isidori, A. (2002). Output regulation of nonlinear systems. *IEEE Transactions on Automatic Control*, 35(2), 131–140.

Chen, X.L. and Liu, Y.J. (2014). *Finite element modeling and simulation with ANSYS workbench.*

Cox, N., Marconi, L., and Teel, A.R. (2011a). Hybrid output regulation with unmeasured clock. In *IEEE Conference on Decision and Control(CDC) and European Control Conference(ECC)*, 7410–7415.

Cox, N., Marconi, L., and Teel, A.R. (2012). Hybrid internal models for robust spline tracking. In *IEEE Conference on Decision and Control(CDC)*, 4877–4882.

Cox, N., Marconi, L., and Teel, A.R. (2016). Isolating invisible dynamics in the design of robust hybrid internal models. *Automatica*, 68, 56–68.

Cox, N., Teel, A., and Marconi, L. (2011b). Hybrid output regulation for minimum phase linear systems. In *American Control Conference*, 863–868.

Francis, B. and Wonham, W.M. (1976). The internal model principle of control theory. *Automatica*, 12(5), 457–465.

Francis, B.A. (1975). The linear multivariable regulator problem. *Siam Journal on Control and Optimization*, 15(3), 873–878.

Goebel, R., Sanfelice, R., and Teel, A.R. (2012). *Hybrid dynamical systems: Modeling, Stability, and Robustness.* Princteon, NJ, USA: Princeton Univ. Press.

Guo, Y., Wang, L., Zhu, Q., Liao, C., and Fang, L. (2016). Switch-on modeling and analysis of dynamic wireless charging system used for electric vehicles. *IEEE Transactions on Industrial Electronics*, 63(10), 6568–6579.

Hwang, K., Cho, J., Kim, D., Park, J., Kwon, J., Sang, K., Park, H., and Ahn, S. (2017). An autonomous coil alignment system for the dynamic wireless charging of electric vehicles to minimize lateral misalignment. *Energies*, 10(3), 315–.

Isidori, A., Marconi, L., and Serrani, A. (2003). *Robust Autonomous Guidance - An Internal Model Approach.* Springer Verlag.

Li, W., Mi, C.C., Li, S., Deng, J., Kan, T., and Han, Z. (2015). Integrated lcc compensation topology for wireless charger in electric and plug-in electric vehicles. *IEEE Transactions on Industrial Electronics*, 62(7), 4215–4225.

Lovison, G., Kobayashi, D., Sato, M., Imura, T., and Hori, Y. (2017). Secondary-side-only control for high efficiency and desired power with two converters in wireless power transfer systems. *Ieej Journal of Industry Applications*, 6(6), 473–481.

Marconi, L. and Teel, A.R. (2013). Internal model principle for linear systems with periodic state jumps. *IEEE Transactions on Automatic Control*, 58(11), 2788–2802.

Marconi, L. and Teel, A.R. (2010). A note about hybrid linear regulation. In *IEEE Conference on Decision and Control.*

Qiang, Z., Huang, Y.X., Niu, T.L., and Xu, C.Y. (2017). Analysis and control of dynamic wireless charging output power for electric vehicle. In *International Conference on Intelligent Computation Technology and Automation.*

Rakhymbay, A., Khamitov, A., Bagheri, M., Alimkhanuly, B., Lu, M., and Phung, T. (2018). Precise analysis on mutual inductance variation in dynamic wireless charging of electric vehicle. *Energies*, 11(3), 624.

Schumaker, L. (2007). *Spline functions:basic theory.* Cambridge Mathematical Library 3rd Edition.

Suntio, T. (2009). *Dynamic Profile of Switched-Mode Converter: Modeling, Analysis and Control.*